HHS Public Access

Author manuscript

Brain Struct Funct. Author manuscript; available in PMC 2018 January 01.

Published in final edited form as:

Brain Struct Funct. 2017 July ; 222(5): 2405–2419. doi:10.1007/s00429-016-1349-z.

Acute restraint stress decreases c-fos immunoreactivity in hilar mossy cells of the adult dentate gyrus

Jillian N. Moretto[1], **Áine M. Duffy**[1], and **Helen E. Scharfman**[1,2]

[1]The Nathan Kline Institute of Psychiatric Research, Orangeburg, NY 10962, USA

[2]Departments of Child and Adolescent Psychiatry, Physiology and Neuroscience, and Psychiatry, New York University Langone Medical Center, New York, NY 10016, USA

Abstract

Although a great deal of information is available about the circuitry of the mossy cells (MCs) of the dentate gyrus (DG) hilus, their activity in vivo is not clear. The immediate early gene c-fos can be used to gain insight into the activity of MCs in vivo, because c-fos protein expression reflects increased neuronal activity. In prior work, it was identified that control rats that were perfusion-fixed after removal from their home cage exhibited c-fos immunoreactivity (ir) in the DG in a spatially stereotyped pattern: ventral MCs and dorsal granule cells (GCs) expressed c-fos protein (Duffy et al., Hippocampus 23:649–655, 2013). In this study, we hypothesized that restraint stress would alter c-fos-ir, because MCs express glucocorticoid type 2 receptors and the DG is considered to be involved in behaviors related to stress or anxiety. We show that acute restraint using a transparent nose cone for just 10 min led to reduced c-fos-ir in ventral MCs compared to control rats. In these comparisons, c-fos-ir was evaluated 30 min after the 10 min-long period of restraint, and if evaluation was later than 30 min c-fos-ir was no longer suppressed. Granule cells (GCs) also showed suppressed c-fos-ir after acute restraint, but it was different than MCs, because the suppression persisted for over 30 min after the restraint. We conclude that c-fos protein expression is rapidly and transiently reduced in ventral hilar MCs after a brief period of restraint, and suppressed longer in dorsal GCs.

Keywords

Hilus; Hippocampus; Interneuron; Granule cell

Introduction

Hilar mossy cells (MCs) of the dentate gyrus (DG) are a common hilar cell type (Buckmaster and Jongen-Relo 1999; Jiao and Nadler 2007; Volz et al. 2011), and the only glutamatergic cell type in the DG other than the primary cell type, the granule cells (GCs, Soriano and Frotscher 1994; Amaral et al. 2007). A great deal is known about MCs in terms of their structure and connectivity (Scharfman and Myers 2012). Their cell bodies are located only in the hilus, and their dendrites are located primarily in the hilus (Amaral 1978;

Correspondence to: Helen E. Scharfman.

Ribak et al. 1985; Frotscher et al. 1991; Scharfman 1991; Blackstad et al. 2016). They receive diverse sources of afferent input from hippocampal neurons (GCs, interneurons, and pyramidal cells, Amaral 1978; Ribak et al. 1985; Frotscher et al. 1991; Scharfman 1994; Acsady et al. 2000) and extrahippocampal input (Deller et al. 1999; Scharfman and Myers 2012; Walling et al. 2012). Their axon forms the commissural-associational projection to the inner molecular layer (IML) of the DG where synapses are made on GCs primarily (Buzsaki and Eidelberg 1981; Laurberg and Sorensen 1981; Ribak et al. 1985; Frotscher et al. 1991; Buckmaster et al. 1996; Wenzel et al. 1997). MCs innervate diverse types of DG interneurons, particularly the perisomatic-targeting subtype known as the basket cell (Sloviter 1991; Buckmaster et al. 1996; Scharfman and Myers 2012).

In contrast to what is known about their connectivity, very little is understood about MC activity in vivo. One of the gaps in our understanding is how behavioral stress affects MCs. This is potentially important, because behavioral stress clearly influences the DG (Fa et al. 2014; Reul et al. 2015; de Kloet and Molendijk 2016; McEwen et al. 2016) and MCs are highly interconnected with other DG neurons with axons that project to local and distant locations of the DG (see also Scharfman and Myers 2012; Scharfman 2016). Therefore, if MCs were affected by stress, they could readily influence other DG neurons throughout the septotemporal axis. However, whether MCs contribute to the response of the DG to stress is not known. One would think that MCs might be involved in stress responses, because they have glucocorticoid type 2 receptors, like DG GCs (Patel and Bulloch 2003). In addition, MCs usually have a low threshold for action potential generation in response to afferent input and can remain depolarized (Scharfman and Schwartzkroin 1989; Scharfman 1991; Strowbridge and Schwartzkroin 1996). Therefore, they could respond in a robust manner to small changes in the environment that are accompanied by altered afferent input from inside or outside the hippocampus. This idea is consistent with the innervation of MCs by many intrinsic and extrinsic afferent pathways (Scharfman 2016). Data in support of the hypothesis that MCs are highly and rapidly responsive to environmental changes have been published (Duffy et al. 2013). In that study, MCs showed increased c-fos protein expression when animals were simply removed from their home cages (Duffy et al. 2013). These findings led to the hypothesis that MCs act as environmental sensors or sentinels in the DG which signal to other DG neurons that are typically harder to activate, such as GCs (Scharfman 2016). This potential function of MCs might be important when the environment becomes dangerous, which typically invokes behavioral stress. Although effects of stress on MCs have not been directly tested, there is indirect support for the idea that brief behavioral stress would influence MCs, because a 15 min-long period of forced swim stress decreased commissural inhibition in the DG (Yarom et al. 2008). Commissural inhibition is the inhibition of DG GCs by a stimulus to the contralateral DG or commissure connecting the two hippocampi, and is mediated by contralateral projecting axons of DG neurons, most of which are MCs (Buzsaki and Eidelberg 1981; Douglas et al. 1983; Scharfman and Myers 2012; Scharfman 2016).

In summary, the goal of the study was to test the hypothesis that c-fos protein expression in MCs would rapidly change in response to brief behavioral stress. In addition, we asked if the changes in MCs would be accompanied by changes in the DG GCs and interneurons, because that would further support the hypothesis that MCs are involved in the response to

stress of other DG neurons that may be relatively unresponsive to afferent input. Because forced swim stress is a complex set of conditions, we chose a simpler method to induce behavioral stress, i.e., restraint using a nose cone or a small transparent enclosure. Animals were placed in a new cage and restrained for 10 min using a nose cone or plastic box. Then, they were perfused after a delay of 30 min or more, to allow for c-fos protein synthesis. Comparisons were made to rats that were placed in a new cage but not restrained, or other control procedures. To analyze the results, the entire septotemporal axis was examined for c-fos immunoreactivity (ir) and other markers. The results showed that acute restraint suppressed ventral MC c-fos-ir compared to controls, and dorsal GC c-fos-ir was greatly reduced also. Interestingly, the MC c-fos-ir was not suppressed if the delay between restraint and perfusion was >30 min, suggesting a transient effect of restraint on MCs. In contrast, GC c-fos-ir was suppressed for longer periods of time. We conclude that acute restraint suppresses MC c-fos-ir with a brief timecourse, but this is not the case for GCs. These data support the hypothesis that MCs are highly responsive to changes in the environment and participate in the response to stress of the DG.

Methods

General procedures

All procedures were approved by the Institutional Animal Care and Use Committee at The Nathan Kline Institute. Care was taken to minimize animal use where possible and reduce discomfort of any kind. Reagents were from Sigma-Aldrich (St. Louis, MO, USA) unless otherwise stated.

Animals

Adult male Sprague-Dawley rats (50–90 days) were bred in-house from animals purchased from Charles River (Kingston, NY, USA). They were maintained in standard cages with food (Purina 5001, W.F. Fisher, NJ, USA) and water ad libitum and a 12 h light–dark cycle.

Behavior

Animals were used between 10:00 a.m. and 2:00 p.m. Pairs of rats were housed together since weaning, and one cage was brought to the laboratory at one time. The cage was placed on a standard laboratory bench with a cage cover to shield it from direct light. The cage holders for food and a water bottle were kept in place. Only one animal was used from each cage; the other was not used for any experiments.

In the restraint group, one animal was removed from the home cage, placed in the center of a new cage with fresh bedding, with a cage cover. A soft plastic nose cone (DecapiCone, Braintree Scientific, Inc., Braintree, MA, USA) was positioned so the body was inside the nose cone, with the nose outside the small end, so the animal could breathe freely. The cone was secured on the other end with a standard binder clip, without clipping any of the animal (e.g., its fur was not clipped). The tail emerged from the opening that was clipped, so it could move freely. Care was taken to secure the nose cone so that limbs were not possible to move, but they were not bent in an awkward position. The animal was placed in the center of the new cage in the nose cone, and the cage cover returned to its normal position. After 10

min, the binder clip was released and the nose cone removed from the cage. The animal was allowed to move freely in the cage for 30 min and then it was perfusion-fixed.

There were three control groups. Control group 1 had no restraint or new cage; these animals were housed in pairs in their home cage until perfusion. At that time, one animal was removed and perfused (Fig. 2a). The other animal was never used. Control group 2 had no restraint or new cage, but the cagemate was removed after the cage was brought to the laboratory, so the animal was isolated. It was perfused 40 min later (Fig. 2a). Rats in control group 3 were treated the same as the animals that were restrained, being placed in a new cage, isolated from their cagemate. However, the isolated animal was not placed in a nose cone for 10 min. It was perfused after 40 min (Fig. 2a).

To optimize comparisons of c-fos-ir, animals from different experimental groups were processed together. Because so many sections were involved (20/rat), all animals could not be processed at one time. Therefore, one animal from each group (e.g., for Fig. 2, there were four groups) was processed in a single batch, and then batches were repeated until there were at least three animals per group. During these repeated procedures, the reactions were stopped at a similar time, when the DAB reaction was a similar intensity (using a wet mount to check the intensity with a light microscope). Results were averaged. For confocal microscopy, animals from different groups were also processed together in batches, and sections were incubated in reagents for the same length of time.

Perfusion-fixation and sectioning

Animals were placed on a perforated ceramic plate in a glass jar with isoflurane (Aerrane; Baxter)-soaked cotton below the plate. The animal was removed when it lost its righting reflex and injected with an overdose of urethane (2.5 g/kg, i.p.). After deep anesthesia, the abdominal cavity was opened, the pericardial wall reflected, and a small incision was made to the left ventricle for insertion of a perfusion needle, which was clamped in place with a hemostat. Saline (0.9% NaCl in dH_2O) was infused by gravity feed and the right atria were clipped. After 3 min, perfusion was switched to 4% paraformaldehyde diluted in 0.1 M Tris buffer (pH 7.4) for 5 min, and the animal was then placed in a plastic bag and refrigerated for at least 2 h. The brain was removed and post-fixed 1–2 days at 4 °C.

The brain was sectioned (50 μm-thick sections) using a vibratome (Model 1000P; Rankin Biomedical Inc., Lawrence, KS, USA). For each animal, one hemisphere was cut in the coronal plane and the other hemisphere was cut horizontally. Coronal sections from the first hemisphere were used to examine the dorsal DG and horizontal sections from the second hemisphere were used to examine the ventral DG (Fig. 1). Sections were stored in 0.1 M Tris buffer at 4 °C until processing, which occurred within 4 days of sectioning.

Immunohistochemistry

Every sixth section was selected; distances between sections were 300 μm. The first section in the coronal plane was chosen from the part of the septal pole where both blades of the dentate gyrus first come together (similar to −2.9 mm from Bregma in the atlas of Paxinos and Watson 2007; Fig. 1a). Six sections were selected, with the last taken just before the hippocampus curves laterally and begins to descend ventrally (−4.1 mm from Bregma;

Paxinos and Watson 2007; Fig. 1a). The first section in the horizontal plane was chosen from the temporal pole at the first point where the GCL can be readily defined as a ‘c’ shaped layer, corresponding to approximately 2.2 mm above the interaural line in Paxinos and Watson (2007) (Fig. 1b). Fourteen sections were selected, with the last taken at dorsal levels (Fig. 1b).

For brightfield microscopy, a goat polyclonal antibody to c-fos was visualized with 3,3-diaminobenzidine (DAB). To determine whether the c-fos-labeled cells were MCs, double-labeling was performed with a second antibody visualized with NovaRed (Vector). The second antibody, to the glutamate receptor subunit GluR2/3, is expressed by MCs (Leranth et al. 1996). Information about antibodies are listed in Table 1.

Tissue processing was conducted at room temperature with continuous agitation on a rotator, and all incubations were followed by three washes in 0.1 M Tris buffer for 5 min (each) unless otherwise specified. Initially sections were washed in 0.1 M Tris buffer, and incubated in 1% hydrogen peroxide (Fisher Scientific) in 0.1 M Tris buffer for 5 min, to block endogenous peroxides. After washes, sections were incubated for 10 min, first in Tris A (0.25% Triton X-100 in 0.1 M Tris buffer) and then Tris B (0.25% Triton X-100 and 0.005% bovine serum albumin in 0.1 M Tris buffer). Sections were blocked in serum (Table 1) for 1 h to minimize nonspecific bindingof reagents. Sections were then washed again in Tris A (10 min) and Tris B (10 min).

Sections were incubated for 24 h in the primary antiserum (Table 1) at 4 °C, and subsequent procedures were conducted at room temperature. Following a 10 min wash in Tris A, sections were washed for 10 min in Tris B, and then incubated in the secondary antibody (Table 1) for 1 h and subsequently washed for 10 min in Tris A followed by 10 min in Tris B. Then sections were placed in avidin–biotin–horseradish peroxidase complex (ABC) solution (Vectastain Elite Kit, Vector Laboratories) diluted 1:100 in Tris B for 2 h. Following washes in 0.1 M Tris buffer, slices were incubated in 0.022% DAB, (dissolved in 0.1 M Tris), 1 mM $NiCl_2$, 0.2% NH_4Cl, 0.1% glucose oxidase, and 0.8% D(+)-glucose in 0.1 M Tris buffer. $NiCl_2$, NH_4Cl, glucose oxidase, and D(+)-glucose were dissolved in distilled water (dH_2O) and stored in aliquots at 4 °C. The reaction was stopped by washing sections in 0.1 M Tris buffer. Sections were then washed in 0.1 M Tris buffer and mounted on subbed slides. Slides were allowed to dry overnight, and then were dehydrated in a graded series of ethanol (5 min 70% ethanol, 5 min 95% ethanol, and 10 min 100% ethanol), cleared in xylene for 10 min, and then coverslipped with Permount (Fisher Scientific).

For double-labeling with antibodies to c-fos and GluR2/3 (Fig. 3), sections were first incubated with the goat polyclonal c-fos antibody (Table 1) and visualized using DAB as described above (see also Duffy et al. 2013). Following washes, sections were incubated with blocking serum for GluR2/3 (Table 1), and incubated for 24 h with a rabbit polyclonal antibody to GluR2/3 (Table 1). The sections were then incubated in the secondary antibody and biotinylated goat anti-rabbit IgG diluted in Tris B (1:400; Vector Laboratories, Burlingame, CA, USA) for 1 h. Immunoreactivity was visualized with NovaRed (per manufacturer’s instructions; Vector).

All slides were analyzed using a brightfield microscope (BX51, Olympus, Hauppauge, NY, USA), photographed using a digital camera (Retiga 2000R, Q Imaging, Surrey, BC, Canada), and acquired using ImagePro (Media Cybernetics, Bethesda, MD, USA). All settings for the camera (e.g., exposure time) and microscope settings (e.g., lighting) remained the same when photographing sections for the figures. Adobe Photoshop (v. 7.0; Adobe, Redmond, WA, USA) was used to assemble figures.

Immunofluorescence

For confocal microscopy, c-fos was visualized by a fluorescein-labeled antibody and the second antibody (GluR2/3, GAD67, PV, NPY, calretinin, nNOS; Figs. 2, 3) was labeled with a rhodamine-tagged antibody (Table 1) using methods described previously (Barouk et al. 2011; Duffy et al. 2013). Briefly, all sections were washed in 0.1 M phosphate buffer (PB) and blocked in 10% donkey serum (Sigma, St. Louis, MO) in 0.25% Triton and 0.005% BSA in 0.1 M PB for 1 h. The sections were then incubated in the goat polyclonal c-fos antibody (Table 1) and either the antibody to GluR2/3, GAD67, PV, NPY, calretinin, or nNOS (Table 1) in 1% donkey serum and 0.25% Triton X-100 in 0.1 M PB for 24 h. Following primary antibody incubation and 3 × 5 min washes in 0.1 M PB, sections were incubated for 2 h in the secondary antibodies (Table 1). Subsequent to rinses in 0.1 M PB, sections were mounted on glass slides and coverslipped with Prolong Gold antifade reagent (Invitrogen, Carlsbad, CA, USA). Confocal microscopy was performed using an LSM 510 Meta (Zeiss, Carl Zeiss Microimaging, Thornwood, NY, USA), equipped with 488 and 546 mm lasers and LSM 510 Meta Software (Zeiss).

Quantification

Cells were counted manually at 10×–80×. Double-labeled cells were counted if the nucleus and cytoplasm were brought into focus in the same focal plane at 80× (brightfield) or using 1 μm optical sections (confocal).

Corticosteroid ELISA

Trunk blood samples were collected 10 min into each procedure (n = 3/group). For example, in the restraint group, animals were euthanized immediately after 10 min of restraint. Euthanasia was conducted by decapitation with a small animal guillotine (Stoelting) after deep anesthesia using isoflurane inhalation (as described above). The time from removal of the rat from its cage to decapitation was less than 60 s. Blood was collected into 15 ml centrifuge tubes and centrifuged at 2000 rotations per min (RPM) for 10 min at room temperature. Serum was removed with a Pasteur pipette, using a new pipette for each tube. Serum was placed into Eppendorf tubes and stored at −80 °C. ELISA was conducted according to the manufacturer's instructions (Alpco mouse and rat corticosterone ELISA, Alpco, Salem, NH, USA).

Statistics

Results are reported as mean ± standard error of the mean (SEM) and the p criterion was 0.05. Statistical comparisons were conducted in Prism (Graphpad, San Francisco, CA, USA) for two-way repeated measures ANOVA (two-way RMANOVA), one-way ANOVA, or

Student's *t* tests, which were two-tailed. When there was inhomogeneity of variance, a constant was added to each data point and the data were log-transformed prior to statistical analysis (Zivin and Bartko 1976). ANOVAs were followed by Tukey–Kramer post hoc tests.

Results

Nose cone restraint decreases hilar c-fos-ir

Figure 2 shows quantitative comparisons of all four groups (restraint and control groups 1–3; see Methods and Fig. 2a), where c-fos-ir cells are plotted with respect to their position along the septotemporal axis. For the hilus, cells with c-fos-ir were found exclusively in ventral DG (Fig. 2b1). A two-way RMANOVA showed a significant effect of group ($F(3,9)6.90$, $p = 0.010$). There also was a significant effect of septotemporal level ($F(19,171)16.53$, $p < 0.0001$), reflecting that hilar c-fos-ir was predominantly in the ventral DG. There was a significant interaction of factors ($F(57,171)2.13$, $p < 0.0001$), with group differences only evident in the ventral sections (Fig. 2b1).

After conducting the two-way RMANOVA for all four groups, we compared restrained rats to each of the control groups. Restrained rats vs. rats from control group 1 showed a significant effect of group ($F(1,4)22.67$, $p = 0.0089$), septotemporal level ($F(19,76)11.25$, $p < 0.0001$), and interaction ($F(19,76)7.42$, $p < 0.0001$). For restraint vs. control group 2, there was also an effect of group ($F(1.5)7.13$, $p < 0.0001$), septotemporal level ($F(19,95)8.27$, $p < 0.0001$), and interaction ($F(19,95)3.79$, $p = 0.044$). For the comparison of restraint to control group 3, the effect of group was close to significance ($F(1,4)6.74$, $p = 0.060$), there was an effect of septotemporal level ($F(19,76)2.60$, $p = 0.0017$) and no interaction ($F(19,76)1.20$, $p = 0.2797$). Thus, restrained rats were significantly different from control groups 1 and 2 but not 3. Presumably, this is because there is some effect of the new cage and isolation as well as restraint on c-fos protein expression, with control group 3 having the new cage and isolation, so it was most similar to the restraint group.

Although there was a prominent septotemporal variation in hilar c-fos under all conditions, the group differences were robust enough to be evident when sections were pooled. Thus, pooled data for each animal (Fig. 2c1) showed significant group differences by one-way ANOVA ($F(3,9)6.90$, $p = 0.010$). Post-hoc comparisons showing that the restrained animals were significantly different from control group 1 (post hoc test, $p < 0.05$), but not control groups 2–3 (post hoc tests, $p > 0.05$). Thus, pooling showed an effect, but it was less sensitive. For this reason, results described in subsequent figures focused on plotting data in relation to the septotemporal axis.

Nose cone restraint reduces GCL c-fos-ir

In Fig. 2b2, c-fos labeling in the GCL is plotted. The majority of labeled cells were in the dorsal DG, consistent with prior findings of control rats (Duffy et al. 2013). The restrained group had low values (Fig. 2b2). There was a significant effect of group ($F(3,9)16.61$, $p = 0.0005$) and septotemporal level ($F(19,171)8.48$, $p < 0.0001$) by two-way RMANOVA, and there was an interaction ($F(57,171)1.43$, $p = 0.042$) reflecting that the reduction in c-fos-ir was primarily in the dorsal DG (Fig. 2b2).

In paired comparisons, the restrained group was significantly different from control group 1, where there was an effect of group (two-way RMANOVA; $F(1,4)46.44$, $p = 0.002$), septotemporal level ($F(19,76)8.07$, $p < 0.0001$), and interaction ($F(19,76)2.17$, $p = 0.010$). For restrained vs. control group 2 rats, the group differences were close to significant ($F(1,4)5.90$, $p = 0.059$), and there was a septotemporal effect ($F(19,95)3.93$, $p < 0.0001$) and no interaction ($F(19,95)0.54$, $p = 0.932$). The restrained rats were different from control group 3, where there was an effect of group ($F(1,4)32.4$; $p = 0.005$), septotemporal level ($F(19,76)4.06$, $p < 0.0001$) but no interaction ($F(19,76)1.44$, $p = 0.135$). In summary, GCs showed reduced c-fos-ir after restraint and the difference was primarily when restrained rats were compared to control groups 1 and 3.

When GCs were pooled from different from septotemporal levels (Fig. 2c2), GCL c-fos-ir was significantly different from control group 3 by one-way ANOVA ($F(3,9)4.382$, $p = 0.0367$; Fig. 2c2). In summary, dorsal GCL c-fos-ir and ventral hilar c-fos-ir were reduced by acute restraint. When all data were analyzed with respect to the septotemporal axis, hilar c-fos-ir showing significant differences between restraint and control groups 1 and 2 and GCL c-fos-ir showed differences between restraint and control groups 1 and 3. Distinctions between hilar and GCL c-fos-ir were also found in their time course, as described below.

Confirmation that hilar c-fos-ir is primarily localized to MCs and GCL c-fos-ir is primarily in GCs

It has been shown that hilar c-fos-ir is primarily in ventral DG in the previous studies using the conditions that we use here for control animals (Duffy et al. 2013). In the previous study, 100% of the hilar cells that exhibited c-fos-ir co-expressed GluR2/3 (Duffy et al. 2013). These data suggested that all c-fos-ir neurons in the hilus were MCs, because MCs represent almost all of the glutamatergic neurons of the hilus. The other cells are ectopic GCs and quite rare compared to MCs (McCloskey et al. 2006). These data were surprising, because there are many GABAergic neurons in the hilus and they did not seem to express c-fos protein. However, MCs and GCs innervate those neurons, and they receive afferent input from outside the DG as well. Because those results were surprising, we looked again in two rats. One of these rats was from control group 1 and the other from the restrained group (Fig. 3). Five sections from the ventral DG were selected per rat. Out of 236 hilar cells labeled with c-fos, all were double-labeled except 3 in the control rat and 1 in the restrained rat (4/236 or 1.7%). Therefore, almost all hilar c-fos-ir cells were GluR2/3-ir and are likely to be MCs.

In the same prior study (Duffy et al. 2013), the dorsal DG rarely showed hilar c-fos-ir, but there was scattered c-fos-ir cells in the GCL. It was reported that these c-fos-ir cells failed to double-label with interneuron markers PV and NPY, so it was concluded that the c-fos-ir cells were GCs (Duffy et al. 2013). In this study, we also found no double-labeling using PV and NPY in the dorsal GCL of rats that were either controls or restrained, and there also was no double-labeling with other interneuron markers (GAD67, calretinin, or nNOS), despite the presence of robust labeling independent of c-fos-ir (Fig. 4). Therefore, we interpret the c-fos-ir labeling in the GCL as labeling of GCs.

Effects of restraint on c-fos-ir are influenced by delay to perfusion-fixation

We next asked if the suppression of c-fos-ir by restraint would be different if the time to perfusion-fixation was changed. One reason to suspect the delay would influence the results is based on the literature showing that c-fos protein expression has a time course that can last for hours after a stimulus, but does not always do so (Le Gal La Salle 1988; Dragunow and Faull 1989; Collaco-Moraes and De Belleroche 1995; Baille-Le Crom et al. 1996; Zimmer et al. 1997).

To address this issue, we perfused animals at 75 or 120 min after 10 min of restraint and compared them to the rats from Fig. 2b that were perfused 30 min after 10 min of restraint. This approach is diagrammed in Fig. 5a. As with prior results, there was a significant effect of the septotemporal axis, with most labeled cells in ventral DG (Fig. 5b1). A two-way RMANOVA showed a significant effect of delay ($F(2,6)1.04$, $p = 0.408$; Fig. 5b1) and septotemporal level ($F(18,114)9.18$, $p < 0.0001$). The restrained rats that experienced the 30 min delay showed fewest c-fos-ir cells in the hilus (Fig. 5b1). Therefore, the restrained group showed suppression of c-fos-ir that was rapid, being detected when the delay was 30 min but not 75 or 120 min.

In Fig. 5b2, the data are presented for c-fos-ir in the GCL. C-fos expression was low in all groups and did not show significant differences between groups (two-way RMANOVA, $F(2,6)0.410$; $p = 0.681$), although there were septotemporal differences ($F(19,114)6.00$, $p < 0.001$), consistent with greater c-fos-ir in dorsal GCL, in general. There was no interaction of factors ($F(38,114)0.753$, $p = 0.860$). Therefore, the reduction in GCL c-fos protein after acute restraint was persistent, in contrast to hilar c-fos-ir.

Because lengthening the delay to perfusion of restrained rats led to what seemed like control levels of hilar c-fos-ir (compare Figs. 2b1 and 5b1), we asked if this was indeed the case by making statistical comparisons of the results from the restrained rats in Fig. 5b1 to controls. The results, shown in Fig. 6, confirmed that hilar c-fos-ir was not significantly different between restrained and control rats. As diagrammed in Fig. 6a, animals that had been restrained for 10 min and fixed 75 or 120 min later were compared to rats that were placed in a new cage and perfused 85 or 130 min later (Fig. 6a). Two-way RMANOVA showed no significant differences between hilar c-fos-ir for the 75 min delay ($F(1,4)0.00882$, $p = 0.927$). There was a septotemporal difference ($F(18,72)6.831$, $p < 0.001$) with more ventral hilar c-fos-ir than dorsal hilar c-fos-ir, as in other conditions (e.g. Figs. 2b, 5b), but no interaction of factors ($F(16,72)0.841$, $p = 0.647$). Similar results were obtained for the 120 min delay (RMANOVA, effect of restraint: $F(1,4)0.682$, $p = 0.455$, septotemporal level: ($F(18,72)10.36$, $p < 0.0001$, interaction: $F(18,72)0.515$, $p = 0.943$; Fig. 6c, d). Thus, hilar c-fos-ir was transiently expressed in hilar MCs, returning to control values by 75 min.

Increasing the duration of nose cone restraint does not increase the effect of restraint on hilar c-fos-ir

To determine the effects of a longer period of restraint on hilar c-fos-ir, the 10 min restraint period was lengthened to 30 min (Fig. 7). Figure 7a shows that there were two groups, one where rats were placed in a new cage, restrained for 30 min, and perfused 30 min

afterwards, and a second group that was placed in a new cage, had no restraint for 30 min, and was perfused 30 min later.

The results were surprising. For the hilus, a two-way RMANOVA showed that there was no effect of group ($F(1,4)0.47$, $p = 0.532$), although there was an effect of septotemporal level ($F(19,76)6.89$, $p < 0.0001$; Fig. 7b1), consistent with the observations that most hilar c-fos-ir is in ventral DG regardless of condition. There was no interaction of factors ($F(19,76)0.71$, $p = 0.794$), suggesting no significant effects of 30 min restraint when examined 30 min later. These data are consistent with those described above, suggesting that after a short period of time, MC c-fos expression returns to normal. What is very surprising is that this seems to be true even when the restraint continues.

The results for the GCL were also surprising. At first when one examines Fig. 7b, one thinks that the results are similar to the hilus, because there also were no significant differences between the restraint and control groups (effect of group: $F(1,4)3.45$, $p = 0.137$, septotemporal level: $F(19,76)2.46$, $p = 0.030$, and interaction: $F(19,76)0.92$, $p = 0.555$; Fig. 7b2). However, c-fos-ir was depressed for both the control and restrained group compared to the data in Fig. 2b2. The data are consistent with the idea that a long period of a depressed GCL c-fos ir occurs after restraint, partly due to the depression of c-fos-ir after a long time in a new cage and isolation. Although initially there is activation by the new cage and isolation (Fig. 2b2, black), if the animal continues to be in the new cage with isolation, there is reduction in c-fos-ir (Fig. 7b, black). One way to explain this is the new cage activates dorsal GCs, but isolation is a stress that, if persistent, overcomes the activation by novelty and reduces GC c-fos-ir.

Different types of restraint reduce hilar c-fos-ir

To further address the effects of restraint on MCs, a different type of restraint was tested. In this case, a transparent plexiglass box was used to hold the rat rather than a transparent nose cone (Fig. 8a). The rat was enclosed on all sides by the box but could move its body 360 °C, and there was a 1 inch hole on one side to provide air (Fig. 8a). A restraint group ($n = 4$) and control group ($n = 3$) were compared. For the restraint group, a pair of animals was brought to the laboratory, and one was placed in the transparent box for 60 min. The duration of time was long, because the animal was less restrained than in the nose cone. Therefore, we assumed that the restraint might not have been sufficient to induce behavioral stress unless it was prolonged. After 60 min in the box, the rat was placed in a new cage and perfused 30 min later. For the control group, a rat was placed in a new cage for 60 min and perfused 30 min later (Fig. 8a). In this experiment, sections were pooled from each rat (Fig. 8b). The rats that were restrained had less c-fos-ir in the hilus than controls (Student's t test: $t = 3.201$, $df = 5$, $p = 0.0240$; Fig. 8b). Therefore, the effects of a nose cone on hilar c-fos-ir can be obtained with other types of restraint.

Lack of c-fos-ir in DG interneurons

One reason for reduced hilar or GCL c-fos-ir in DG neurons could be that restraint activated GABAergic neurons which increased inhibition of MCs and GCs. Therefore, c-fos-ir was examined in DG interneurons (Fig. 4). Using PV as an interneuron marker, we failed to find

double-labeling of PV and c-fos in rats that were restrained for 10 min and examined 30 min later (Fig. 2a, restraint group). In 3 restrained rats, 6 ventral sections were examined per animal and 221 PV-ir cells were counted. Counts from the GCL and hilus were pooled (mean, 12 cells/section) with no double-labeled cells. We also failed to find double-labeling using NPY as a marker. In this case, 190 cells were examined (mean, 11 cells/section).

Nose cone restraint increases c-fos-ir in the PVN but not serum corticosterone

We assayed corticosterone levels using ELISA to determine whether restrained animals experienced behavioral stress that was sufficient to elevate serum corticosterone levels. For this purpose, a new cohort of rats was used. All groups shown in Fig. 2a were compared (n = 3/group, total 12 rats). Rats were euthanized after 10 min of restraint, 10 min in a new cage, 10 min after removing the cagemate from the home cage, or 10 min after bringing the rat cage to the laboratory (all four groups in Fig. 2a). Serum levels of restrained rats were not significantly different from control groups 1–3 (one-way ANOVA, $F(3,8)1.216$, $p = 0.348$; Fig. 9). One of the possible reasons was that the time of day of our experiments was at the trough of the natural circadian variation in serum corticosterone for male rats, late morning (Zimmer et al. 1997). Our values were comparable to normal levels in rats at this time of day (Reul and de Kloet 1985).

These data were surprising, because they suggested that little stress had been induced by restraint, because serum corticosterone levels were not elevated. Therefore, our procedures probably did induce very mild stress. On the other hand, we observed behavior which suggested that restraint for 10 min produced behavioral stress. For example, animals attempted to move when restrained by the nose cone and defecated in the cage when they were initially restrained. On the other hand, after ~5 min, they appeared to stop attempting to move. To gain more insight, we examined areas of the same brains where we quantified c-fos-ir in the DG. In dorsal coronal sections, we examined the paraventricular nucleus of the hypothalamus (PVN), because it is activated by diverse behavioral stresses (Dragunow and Faull 1989; Collaco-Moraes and De Belleroche 1995; Reul et al. 2015). In coronal sections at approximately 1.7 mm posterior to Bregma, to capture the PVN (Paxinos and Watson 2007), restrained animals showed elevated c-fos-ir in the PVN ($F(3,8)111.5$, $p < 0.0001$; post hoc tests, $p < 0.05$; Fig. 9). These data suggest that stress was induced in the restrained group relative to control groups 1–3, but it was mild, because serum corticosterone levels were not elevated after restraint.

Discussion

The results show that the MCs reduce their expression of c-fos-ir in response to mild restraint stress, and these MCs are in the ventral DG. In response to the nose cone restraint for 10 min, the depression of c-fos-ir in MCs occurred within 30 min, and it was no longer evident if the delay between the stress and perfusion was 60 min or longer. The reduction in c-fos-ir was also absent if the duration of stress was increased from 10 min to 30 min. The results suggest a rapid activation and cessation of c-fos protein synthesis by MCs in response to mild restraint stress.

GCs also had low c-fos protein expression in response to 10 min of restraint, and these GCs were primarily located in the dorsal DG. These GCs showed a robust reduction, lasting for all the delays (to perfusion) that were tested. The GCs also showed an effect of lengthening the restraint, partly due to the fact that prolonging the time in a new cage with isolation depressed GC c-fos-ir. Thus, the regulation of c-fos-ir by behavioral stress is quite different in the MCs and GCs. MCs show sensitivity but rapid changes, and GCs show sensitivity with a slower recovery, as well as effects simply due to movement to a new cage and isolation.

DG interneurons did not seem to be activated, because c-fos protein was not detected in DG interneurons. However, the interneurons could have been active, but not enough to induce c-fos-ir protein expression. Or they could have been quite active, but the pattern of their activity was not appropriate to induce c-fos protein expression. The lack of expression is unlikely to be due to technical problems, because the same methods showed robust c-fos-ir in PV and NPY-expressing interneurons after seizures (Scharfman et al. 2002). We suggest that negative data be interpreted with caution, because it may be that DG interneurons were active but did not express c-fos.

The relationship of MC c-fos-ir to GC c-fos-ir

Ventral mossy cells project to the dorsal DG where their axons terminate primarily in the inner molecular layer; their synapses are primarily on GC dendrites (Buzsaki and Eidelberg 1981; Laurberg and Sorensen 1981; Ribak et al. 1985; Frotscher et al. 1991; Buckmaster et al. 1996; Wenzel et al. 1997). Therefore, the activity of the ventral MCs may stimulate GCs in dorsal DG and be responsible for their c-fos protein synthesis. This idea is supported by prior observations, where increases in ventral MC c-fos-ir correlated with dorsal GC c-fos-ir (Duffy et al. 2013). In addition, if ventral MCs reduce their activity, the activity and c-fos protein expression of dorsal GCs may decrease because of a loss of afferent input from MCs. However, other data suggest a dissociation between MC activity and GC activity. For example, increasing the duration of the delay between restraint and perfusion reduced the effect of restraint for 10 min on c-fos-ir in the hilus, but this did not occur in the GCL. On the other hand, recovery from suppressed c-fos protein expression may simply have a different time course in MCs and GCs. Another reason to suggest that MCs are not responsible for GC c-fos-ir is that lengthening time in a new cage and isolation decreased GC c-fos-ir, but this was not evident in MCs. In summary, dorsal GCs may be influenced by ventral MCs, but they are also influenced by other factors, which is what would be expected, since the MCs only innervate the proximal third of the GC dendritic tree.

The role of MCs in the DG circuitry

The results support the hypothesis that ventral MCs are influenced by stress, which is consistent with the idea that behavioral stress using acute restraint does affect the DG (Herman and Watson 1995; Conrad and McEwen 2000; Fujikawa et al. 2000; Bain et al. 2004; Fevurly and Spencer 2004; Nativio et al. 2012; Hoffman et al. 2013). The data are consistent with Chowdhury et al. (2000) who showed that DG c-fos is decreased after restraint stress in water, and Hoffman et al. (2013) who showed that 6 h of restraint stress led to reduced c-fos in the DG on the next day, when animals were exposed to the environment

of the restraint stress. In a recent study, administration of the glucocorticoid receptor agonist dexamethasone led to decreased activation of dorsal GCs (Law et al. 2016), which is very interesting, because the authors activated the DG by novelty, similar to what our studies suggest activate ventral MCs and dorsal GCs (Duffy et al. 2013). Finally, the data are also consistent with persistent effects of stress on the dentate gyrus (Mizukawa et al. 1989).

The results also suggest a dissociation between the MCs and GCs, because MCs recovered faster than GCs to the same behavioral stress. This finding is consistent with the idea that MCs are rapid sensors of change in the environment, and relay that information to GCs. For this function to be optimal, depression in MC activity should be brief, so that they can be activated readily by the next change in the environment.

This idea of MCs as a sensors or sentinels was originally based on data showing that a subset of MCs have a low threshold for afferent activation by the perforant path in hippocampal slices (Scharfman 1991). In recordings of MCs, they were more easily activated than GCs because of a more depolarized resting potential and ongoing barrage of excitatory afferent input (Scharfman 1993). It has been proposed that MCs could serve an important function in the DG circuit by having a low threshold, because it would allow MCs to be activated by weak EC input that fails to activate most GCs. MCs could ensure that many GCs would be depolarized by the weak EC input. Alternatively, MCs may provide important inhibitory input to GCs by activating DG interneurons to keep GCs inhibited (Sloviter 1991; Jinde et al. 2012; Hsu et al. 2016). Our results do not provide evidence for this hypothesis but as mentioned above, low c-fos-ir in DG interneurons should be interpreted carefully.

It is not clear why c-fos expression was detected mainly in ventral MCs and dorsal GCs, but it seems likely that it is related to the proposed division of functions of the DG, with the dorsal DG associated with ‘cognitive’ functions and the ventral DG related to functions which have a limbic component, i.e., stress or anxiety (Kheirbek et al. 2013; Strange et al. 2014). One possibility is that limbic input to ventral MCs makes the MCs sensitive to stress, and this helps the dorsal GC functions that are cognitive be influenced by stress. This idea is consistent with the fact that stress adversely influences cognitive function (Hölscher 1999).

Summary

Studies of c-fos protein expression have limitations, but the results presented here support two important conclusions, nevertheless: ventral MCs and dorsal GCs are less active after acute restraint. In addition, reduced activity recovers relatively rapidly in MCs compared to GCs.

Acknowledgments

Supported by NIH 090606, the Alzheimer’s Association, and the New York State Office of Mental Health.

References

Acsady L, Katona I, Martinez-Guijarro FJ, Buzsaki G, Freund TF. Unusual target selectivity of perisomatic inhibitory cells in the hilar region of the rat hippocampus. J Neurosci. 2000; 20:6907–6919. [PubMed: 10995835]

Amaral D. A Golgi study of cell types in the hilar region of the hippocampus in the rat. J Comp Neurol. 1978; 15:851–914.

Amaral DG, Scharfman HE, Lavenex P. The dentate gyrus: fundamental neuroanatomical organization (dentate gyrus for dummies). Prog Brain Res. 2007; 163:3–22. [PubMed: 17765709]

Baille-Le Crom V, Collombet JM, Burckhart MF, Foquin A, Pernot-Marino I, Rondouin G, Lallement G. Time course and regional expression of c-fos and HSP 70 in hippocampus and piriform cortex following soman-induced seizures. J Neurosci Res. 1996; 45:513–524. [PubMed: 8875316]

Bain M, Dwyer S, Rusak B. Restraint stress affects hippocampal cell proliferation differently in rats and mice. Neurosci Lett. 2004; 368:7–10. [PubMed: 15342123]

Barouk S, Hintz T, Li P, Duffy A, Maclusky N, Scharfman H. 17β-estradiol increases astrocytic vascular endothelial growth factor (VEGF) in adult female rat hippocampus. Endocrinology. 2011; 152:1745–1751. [PubMed: 21343256]

Blackstad JB, Osen KK, Scharfman HE, Storm-Mathisen J, Blackstad TW, Leergaard TB. Observations on hippocampal mossy cells in mink (neovison vison) with special reference to dendrites ascending to the granular and molecular layers. Hippocampus. 2016; 26:229–245. [PubMed: 26286893]

Buckmaster PS, Jongen-Relo AL. Highly specific neuron loss preserves lateral inhibitory circuits in the dentate gyrus of kainate-induced epileptic rats. J Neurosci. 1999; 19:9519–9529. [PubMed: 10531454]

Buckmaster P, Wenzel H, Kunkel D, Schwartzkroin P. Axon arbors and synaptic connections of hippocampal mossy cells in the rat in vivo. J Comp Neurol. 1996; 366:271–292. [PubMed: 8698887]

Buzsaki G, Eidelberg E. Commissural projection to the dentate gyrus of the rat: evidence for feed-forward inhibition. Brain Res. 1981; 230:346–350. [PubMed: 7317783]

Celio MR. Calbindin D-28 k and parvalbumin in the rat nervous system. Neuroscience. 1990; 35:375–475. [PubMed: 2199841]

Chowdhury GM, Fujioka T, Nakamura S. Induction and adaptation of fos expression in the rat brain by two types of acute restraint stress. Brain Res Bull. 2000; 52:171–182. [PubMed: 10822158]

Collaco-Moraes Y, De Belleroche J. Differential temporal patterns of expression of immediate early genes in cerebral cortex induced by intracerebral excitotoxin injection: sensitivity to dexamethasone and MK-801. Neuropharmacology. 1995; 34:521–531. [PubMed: 7566487]

Conrad C, McEwen B. Acute stress increases neuropeptide Y mRNA within the arcuate nucleus and hilus of the dentate gyrus. Mol Brain Res. 2000; 79:102–109. [PubMed: 10925147]

de Kloet ER, Molendijk ML. Coping with the forced swim stressor: towards understanding an adaptive mechanism. Neural Plasticity. 2016; 2016:6503162. [PubMed: 27034848]

Deller T, Katona I, Cozzari C, Frotscher M, Freund TF. Cholinergic innervation of mossy cells in the rat fascia dentata. Hippocampus. 1999; 9:314–320. [PubMed: 10401645]

Douglas RM, McNaughton BL, Goddard GV. Commissural inhibition and facilitation of granule cell discharge in fascia dentata. J Comp Neurol. 1983; 219:285–294. [PubMed: 6311879]

Dragunow M, Faull R. The use of c-fos as a metabolic marker in neuronal pathway tracing. J Neurosci Methods. 1989; 29:261–265. [PubMed: 2507830]

Duffy AM, Schaner MJ, Chin J, Scharfman HE. Expression of c-fos in hilar mossy cells of the dentate gyrus in vivo. Hippocampus. 2013; 23:649–655. [PubMed: 23640815]

Fa M, Xia L, Anunu R, Kehat O, Kriebel M, Volkmer H, Richter-Levin G. Stress modulation of hippocampal activity–spotlight on the dentate gyrus. Neurobiol Learn Mem. 2014; 112:53–60. [PubMed: 24747273]

Fevurly RD, Spencer RL. Fos expression is selectively and differentially regulated by endogenous glucocorticoids in the paraventricular nucleus of the hypothalamus and the dentate gyrus. J Neuroendocrinol. 2004; 16:970–979. [PubMed: 15667452]

Frotscher M, Seress L, Schwerdtfeger WK, Buhl E. The mossy cells of the fascia dentata: a comparative study of their fine structure and synaptic connections in rodents and primates. J Comp Neurol. 1991; 312:145–163. [PubMed: 1744242]

Fujikawa T, Soya H, Fukuoka H, Alam K, Yoshizato H, McEwen B, Nakashima K. A biphasic regulation of receptor mRNA expressions for growth hormone, glucocorticoid and mineralocorticoid in the rat dentate gyrus during acute stress. Brain Res. 2000; 874:186–193. [PubMed: 10960603]

Herman J, Watson S. Stress regulation of mineralocorticoid receptor heteronuclear RNA in rat hippocampus. Brain Res. 1995; 677:243–249. [PubMed: 7552249]

Hoffman AN, Anouti DP, Lacagnina MJ, Nikulina EM, Hammer RP Jr, Conrad CD. Experience-dependent effects of context and restraint stress on corticolimbic c-fos expression. Stress. 2013; 16:587–591. [PubMed: 23662914]

Hölscher C. Stress impairs performance in spatial water maze learning tasks. Behav Brain Res. 1999; 100:225–235. [PubMed: 10212070]

Hsu T-T, Lee C-T, Tai M-H, Lien C-C. Differential recruitment of dentate gyrus interneuron types by commissural versus perforant pathways. Cereb Cortex. 2016; 26:2715–2727. [PubMed: 26045570]

Jiao Y, Nadler JV. Stereological analysis of Glur2-immunoreactive hilar neurons in the pilocarpine model of temporal lobe epilepsy: correlation of cell loss with mossy fiber sprouting. Exp Neurol. 2007; 205:569–582. [PubMed: 17475251]

Jinde S, Zsiros V, Jiang Z, Nakao K, Pickel J, Kohno K, Belforte JE, Nakazawa K. Hilar mossy cell degeneration causes transient dentate granule cell hyperexcitability and impaired pattern separation. Neuron. 2012; 76:1189–1200. [PubMed: 23259953]

Kheirbek MA, Drew LJ, Burghardt NS, Costantini DO, Tannenholz L, Ahmari SE, Zeng H, Fenton AA, Hen R. Differential control of learning and anxiety along the dorso-ventral axis of the dentate gyrus. Neuron. 2013; 77:955–968. [PubMed: 23473324]

Laurberg S, Sorensen KE. Associational and commissural collaterals of neurons in the hippocampal formation (hilus fasciae dentatae and subfield CA3). Brain Res. 1981; 212:287–300. [PubMed: 7225870]

Law J, Ibarguen-Vargas Y, Belzung C, Surget A. Decline of hippocampal stress reactivity and neuronal ensemble coherence in a mouse model of depression. Psychoneuroendocrinology. 2016; 67:113–123. [PubMed: 26881837]

Le Gal La Salle G. Long-lasting and sequential increase of c-fos oncoprotein expression in kainic acid-induced status epilepticus. Neurosci Lett. 1988; 88:127–130. [PubMed: 3132654]

Leranth C, Szeidemann Z, Hsu M, Buzsáki G. AMPA receptors in the rat and primate hippocampus: a possible absence of glur2/3 subunits in most interneurons. Neuroscience. 1996; 70:631–652. [PubMed: 9045077]

McCloskey DP, Hintz TM, Pierce JP, Scharfman HE. Stereological methods reveal the robust size and stability of ectopic hilar granule cells after pilocarpine-induced status epilepticus in the adult rat. Eur J Neurosci. 2006; 24:2203–2210. [PubMed: 17042797]

McEwen BS, Nasca C, Gray JD. Stress effects on neuronal structure: hippocampus, amygdala, and prefrontal cortex. Neuropsychopharmacology. 2016; 41:3–23. [PubMed: 26076834]

Mizukawa K, Takayama H, Sato H, Ota Z, Haba K, Ogawa N. Alterations of muscarinic cholinergic receptors in the hippocampal formation of stressed rat: in vitro quantitative autoradiographic analysis. Brain Res. 1989; 478:187–192. [PubMed: 2924116]

Nativio P, Pascale E, Maffei A, Scaccianoce S, Passarelli F. Effect of stress on hippocampal nociceptin expression in the rat. Stress. 2012; 15:378–384. [PubMed: 22074385]

Patel A, Bulloch K. Type II glucocorticoid receptor immunoreactivity in the mossy cells of the rat and the mouse hippocampus. Hippocampus. 2003; 13:59–66. [PubMed: 12625458]

Paxinos, G., Watson, C. The rat brain in stereotaxic coordinates. Elsevier Academic Press; New York: 2007.

Preston GA, Lyon TT, Yin Y, Lang JE, Solomon G, Annab L, Srinivasan DG, Alcorta DA, Barrett JC. Induction of apoptosis by c-fos protein. Mol Cell Biol. 1996; 16:211–218. [PubMed: 8524298]

Reul JM, de Kloet ER. Two receptor systems for corticosterone in rat brain: microdistribution and differential occupation. Endocrinology. 1985; 117:2505–2511. [PubMed: 2998738]

Reul JM, Collins A, Saliba RS, Mifsud KR, Carter SD, Gutierrez- Mecinas M, Qian X, Linthorst AC. Glucocorticoids, epigenetic control and stress resilience. Neurobiol Stress. 2015; 1:44–59. [PubMed: 27589660]

Ribak CE, Seress L, Amaral DG. The development, ultrastructure and synaptic connections of the mossy cells of the dentate gyrus. J Neurocytol. 1985; 14:835–857. [PubMed: 2419523]

Scharfman HE. Dentate hilar cells with dendrites in the molecular layer have lower thresholds for synaptic activation by perforant path than granule cells. J Neurosci. 1991; 11:1660–1673. [PubMed: 2045880]

Scharfman HE. Characteristics of spontaneous and evoked EPSPs recorded from dentate spiny hilar cells in rat hippocampal slices. J Neurophysiol. 1993; 70:742–757. [PubMed: 8105038]

Scharfman HE. Evidence from simultaneous intracellular recordings in rat hippocampal slices that area CA3 pyramidal cells innervate dentate hilar mossy cells. J Neurophysiol. 1994; 72:2167–2180. [PubMed: 7884451]

Scharfman HE. The enigmatic mossy cell of the dentate gyrus. Nat Rev Neurosci. 2016; 17:562–575. [PubMed: 27466143]

Scharfman HE, Myers CE. Hilar mossy cells of the dentate gyrus: a historical perspective. Front Neural Circuits. 2012; 6:106. [PubMed: 23420672]

Scharfman HE, Schwartzkroin PA. Protection of dentate hilar cells from prolonged stimulation by intracellular calcium chelation. Science. 1989; 246:257–260. [PubMed: 2508225]

Scharfman HE, Sollas AL, Goodman JH. Spontaneous recurrent seizures after pilocarpine-induced status epilepticus activate calbindin-immunoreactive hilar cells of the rat dentate gyrus. Neuroscience. 2002; 111:71–81. [PubMed: 11955713]

Sloviter RS. Permanently altered hippocampal structure, excitability, and inhibition after experimental status epilepticus in the rat: the “dormant basket cell” hypothesis and its possible relevance to temporal lobe epilepsy. Hippocampus. 1991; 1:41–66. [PubMed: 1688284]

Soriano E, Frotscher M. Mossy cells of the rat fascia dentata are glutamate-immunoreactive. Hippocampus. 1994; 4:65–69. [PubMed: 7914798]

Strange B, Witter M, Lein E, Moser E. Functional organization of the hippocampal longitudinal axis. Nat Rev Neurosci. 2014; 15:655–669. [PubMed: 25234264]

Strowbridge BW, Schwartzkroin PA. Transient potentiation of spontaneous EPSPs in rat mossy cells induced by depolarization of a single neurone. J Physiol. 1996; 494(Pt 2):493–510. [PubMed: 8842007]

Tse Y-C, Lai C-H, Lai S-K, Liu J-X, Yung KKL, Shum DKY, Chan Y-S. Developmental expression of NMDA and AMPA receptor subunits in vestibular nuclear neurons that encode gravity-related horizontal orientations. J Comp Neurol. 2008; 508:343–364. [PubMed: 18335497]

Volz F, Bock HH, Gierthmuehlen M, Zentner J, Haas CA, Freiman TM. Stereologic estimation of hippocampal GluR2/3- and calretinin-immunoreactive hilar neurons (presumptive mossy cells) in two mouse models of temporal lobe epilepsy. Epilepsia. 2011; 52:1579–1589. [PubMed: 21635231]

Walling SG, Brown RA, Miyasaka N, Yoshihara Y, Harley CW. Selective wheat germ agglutinin (wga) uptake in the hippocampus from the locus coeruleus of dopamine-beta-hydroxylase-wga transgenic mice. Front Behav Neurosci. 2012; 6:23. [PubMed: 22654744]

Wenzel HJ, Buckmaster PS, Anderson NL, Wenzel ME, Schwartzkroin PA. Ultrastructural localization of neurotransmitter immunoreactivity in mossy cell axons and their synaptic targets in the rat dentate gyrus. Hippocampus. 1997; 7:559–570. [PubMed: 9347352]

Whisler RL, Chen M, Beiqing L, Carle KW. Impaired induction of c-fos/c-jun genes and of transcriptional regulatory proteins binding distinct c-fos/c-jun promoter elements in activated human t cells during aging. Cell Immunol. 1997; 175:41–50. [PubMed: 9015187]

Yarom O, Maroun M, Richter-Levin G. Exposure to forced swim stress alters local circuit activity and plasticity in the dentate gyrus of the hippocampus. Neural Plasticity. 2008; 2008:194097. [PubMed: 18301720]

Zimmer LA, Ennis M, El-Etri M, Shipley MT. Anatomical localization and time course of fos expression following somaninduced seizures. J Comp Neurol. 1997; 378:468–481. [PubMed: 9034904]

Zivin JA, Bartko JJ. Statistics for disinterested scientists. Life Sci. 1976; 18:15–26. [PubMed: 1250059]

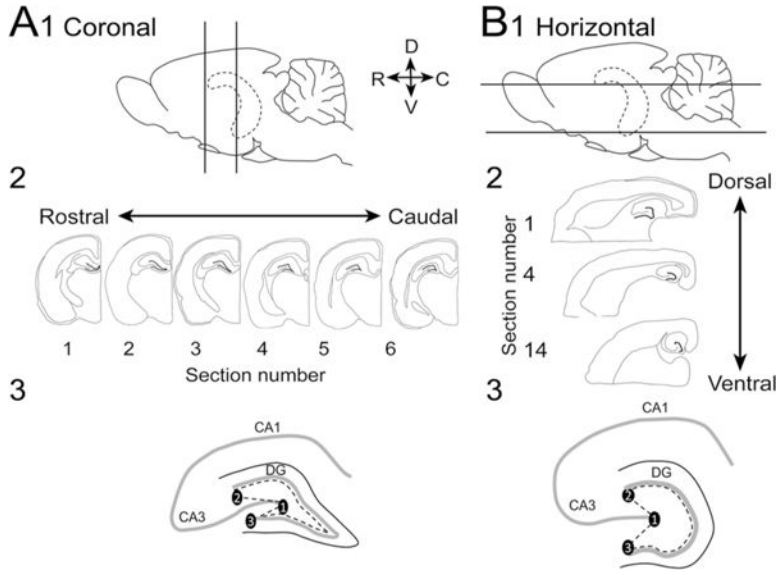

Fig. 1.

Methods used for sectioning and analysis. **a1** Diagram of the brain viewed from the side shows the hippocampus (*dotted lines*) which was cut by sectioning one hemisphere in the coronal plane between the locations indicated by *straight lines*. *D* dorsal, *V* ventral, *R* rostral, *C* caudal. **2** Six sections from the dorsal hippocampus were selected (300 μm apart). **3** A diagram shows how the hilus was defined. Points were connected as follows: *1* lateral tip of the upper blade, *2* end of the pyramidal cell layer, and *3* lateral tip of the lower blade. This line was then connected to another line that outlined the border of the GCL and the hilus. **b1** Diagram of the orientation for horizontal sections. One hemisphere was cut in the coronal plane and the second was cut horizontally. **2** 14 sections from the ventral hippocampus were selected (300 μm apart). **3** A diagram shows how the hilus was defined in horizontal sections

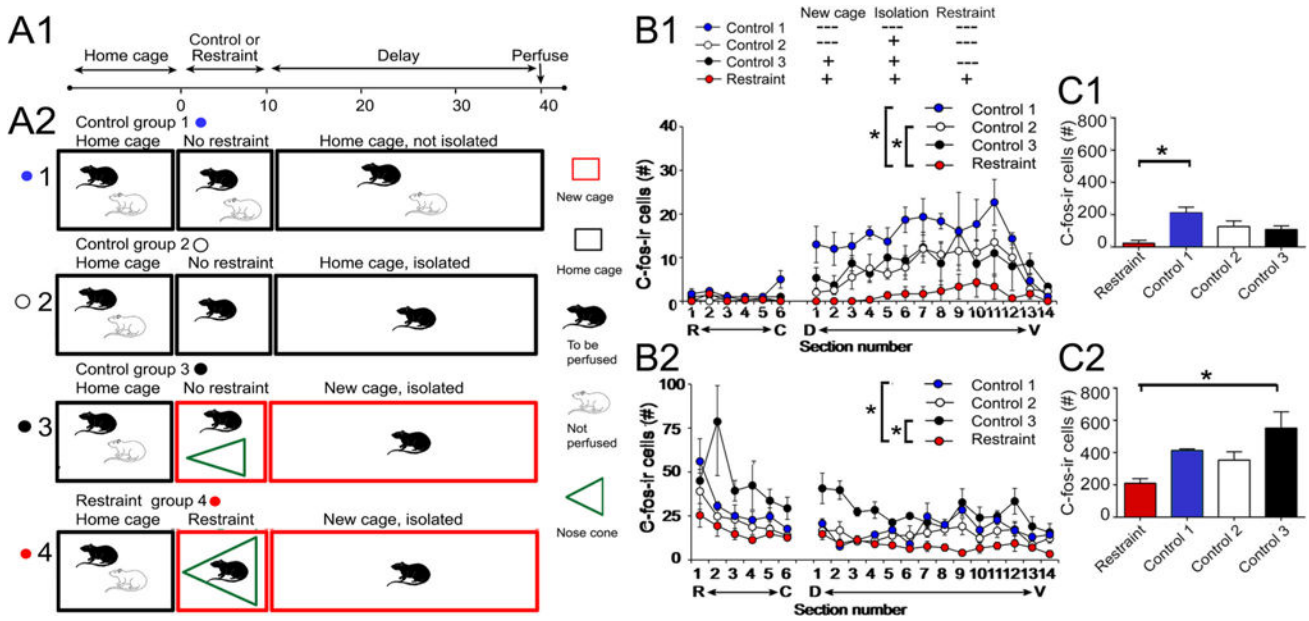

Fig. 2.

Comparison of c-fos-ir in restrained and control rats. **a1** Experimental timeline. Animals were brought to the lab in their home cage, and then they were restrained or were controls. Afterwards, there was a delay of 30 min and then animals were perfusion-fixed. **2** Four experimental groups are shown. All groups started with rats initially housed in pairs, brought to the laboratory in their home cage (*black box*). For control group 1, only one rat of the pair was perfused after 40 min. Control group 2 took one rat out of the home cage when the cage was brought to the lab and the other was perfused 40 min later. Control group 3 took one rat out of the home cage, put it in a new cage, and then perfused it 40 min later. The restrained group took one rat out of the home cage, restrained it in a nose cone (*green*) for 10 min, and then let it move freely for 30 min, when it was perfused. **b1** Mean (±SEM) for hilar c-fos-ir cells is shown for all groups. Sections 1–6 were from the dorsal DG (*R* rostral, *C* caudal, as shown in Fig. 1a). Sections from ventral DG were cut horizontally and the most dorsal section is labeled #1. *D* dorsal, *V* ventral. *Asterisk* indicates significant differences by two-way RMANOVA ($p < 0.05$). The restrained group was significantly different from control groups 1 and 2 by pairwise comparisons ($p < 0.05$). **2** GCL c-fos-ir cells are plotted for all groups. Differences were significant by two-way RMANOVA ($p < 0.05$) with the restrained group significantly different from control groups 1 and 3 by paired comparison ($p < 0.05$). **c1** Hilar c-fos-ir is shown for all four experimental groups. All sections from the septotemporal axis were pooled for each rat. One-way ANOVA showed that there were significant differences ($p < 0.05$). The restrained rats were significantly different from control group 1 (*asterisks*, $p < 0.05$). **2** GCL c-fos-ir is plotted for all groups. The restrained rats were significantly different from control group 3 (*asterisk*, $p < 0.05$)

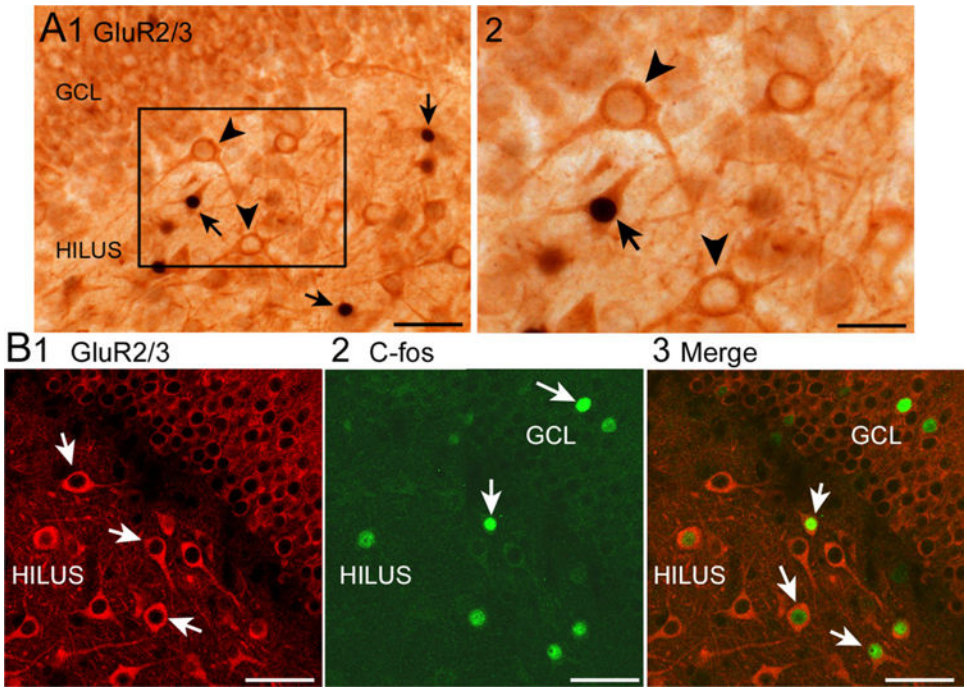

Fig. 3.

C-fos coexpression with GluR2/3 in the hilus. **a** Using brightfield microscopy, cells were labeled first with c-fos using DAB and $NiCl_2$ resulting in black c-fos-ir nuclei. Then, NovaRed was used to label GluR2/3 cells *dark orange*. **1** Double-labeled cells are indicated by the *arrows*; *arrowheads* mark cells that are GluR2/3-labeled but lack c-fos-ir. Calibration, 50 μm. **2** Area outlined by the *box* in **a1** is shown at higher power. Calibration, 25 μm. **b** Using confocal microscopy, cells were labeled with antibodies to GluR2/3 (**1**, *red*) and c-fos (**2**, *green*). **3** Merged image of **1** and **2**. Double-labeled cells are marked by the *arrows*. Calibrations, 50 μm

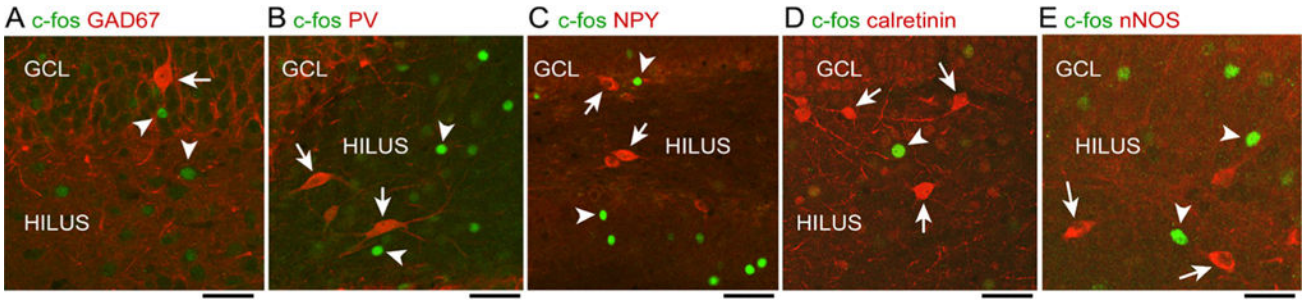

Fig. 4.

C-fos expression without expression of GABergic markers. **a** Cells in the DG that were labeled using an antibody to c-fos (*arrowheads*) were located near cells expressing GAD67 (*arrow*), but there were no double-labeled cells. *GCL* granule cell layer. Calibrations in **a**–**e**, 50 μm. **b** C-fos (*arrowheads*) or parvalbumin (PV; *arrows*)-labeled cells without double-labeling. **c** C-fos (*arrowheads*) or neuropeptide Y (NPY; *arrows*)-labeled cells without double-labeling. **d** C-fos (*arrowhead*) or calretinin (*arrows*)-labeled cells without double-labeling. **e** C-fos (*arrowheads*) or neuronal nitric oxide synthase (nNOS; *arrows*)-labeled cells without double-labeling

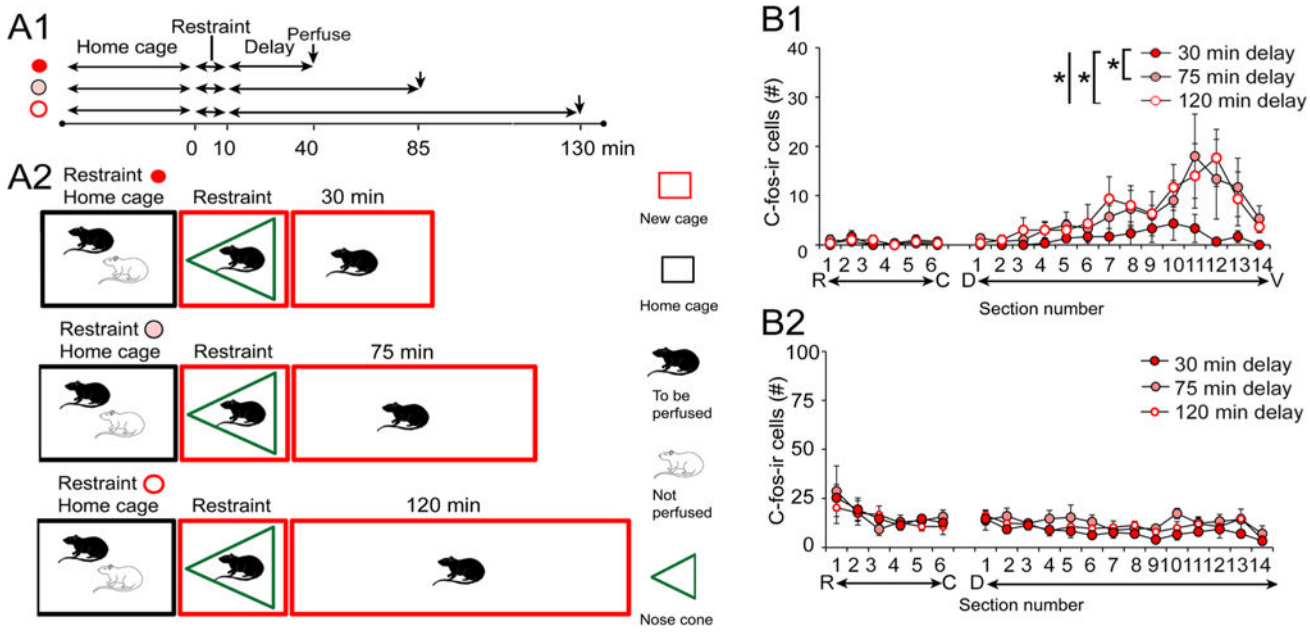

Fig. 5.

Increasing the delay between restraint and perfusion-fixation shows a transient effect of restraint on hilar c-fos-ir. **a** Schematic illustrates the three groups, each having a 10 min period of restraint but different times from restraint to perfusion-fixation. **b1** Graph of hilar c-fos-ir shows that the longer delay to perfusion led to a restoration of hilar c-fos-ir. **b2** GCL c-fos-ir shows that all groups had depressed c-fos-ir

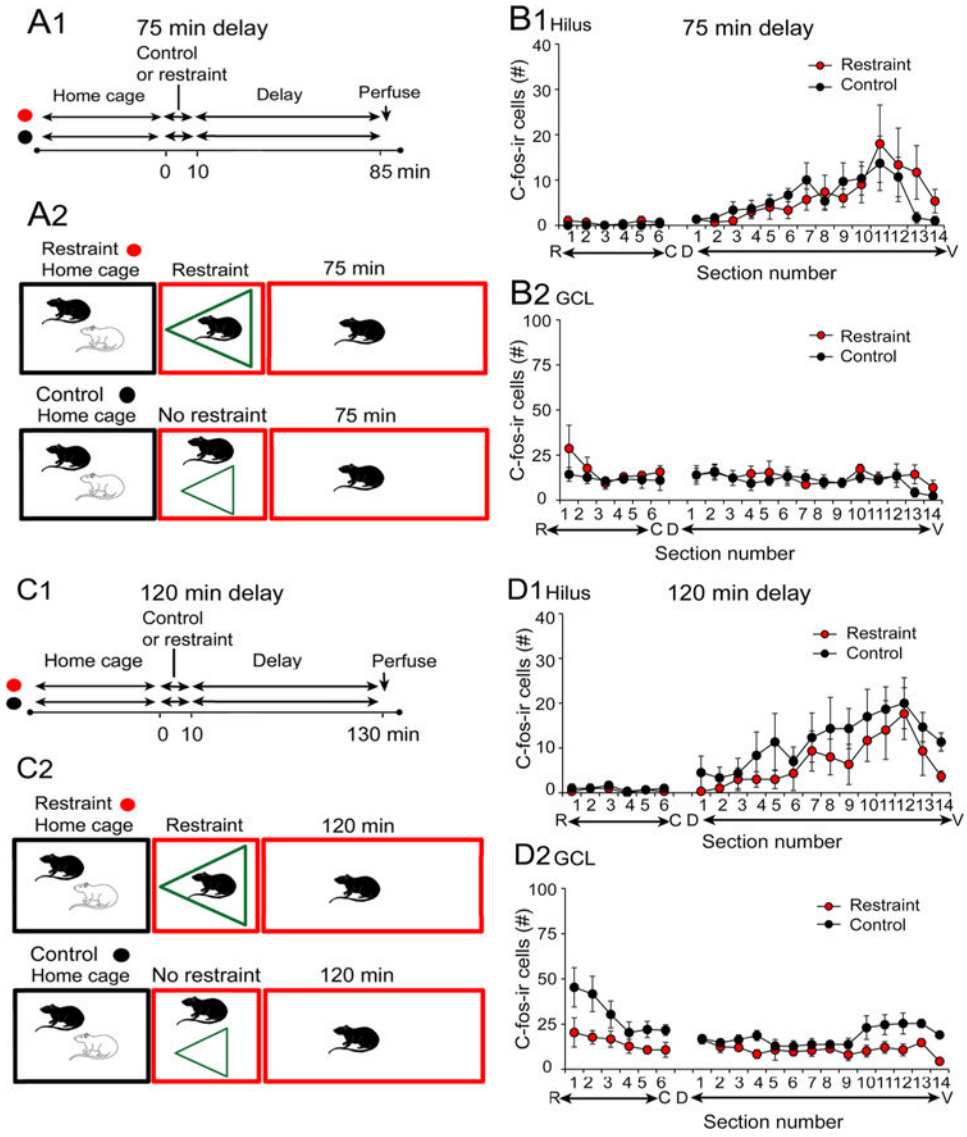

Fig. 6.

Comparisons of different experimental groups with 75 or 120 min delay to perfusion-fixation. **a** Schematic shows the experimental groups in **b**. There was a 10 min period of restraint and then rats were perfused 75 min later (*red*) or the rat was placed in a new cage without its cage mate for 85 min and then was perfused (*black*). **b** Results for hilar and GCL c-fos-ir were similar between the two groups. **c** Schematic shows the experimental groups in **c**. Rats were perfused 120 min after a 10 min period of restraint (*red*) or 130 min after placement in a new cage, isolated from its cagemate (*black*). **d** Results for hilar and GCL c-fos-ir were similar between the two groups

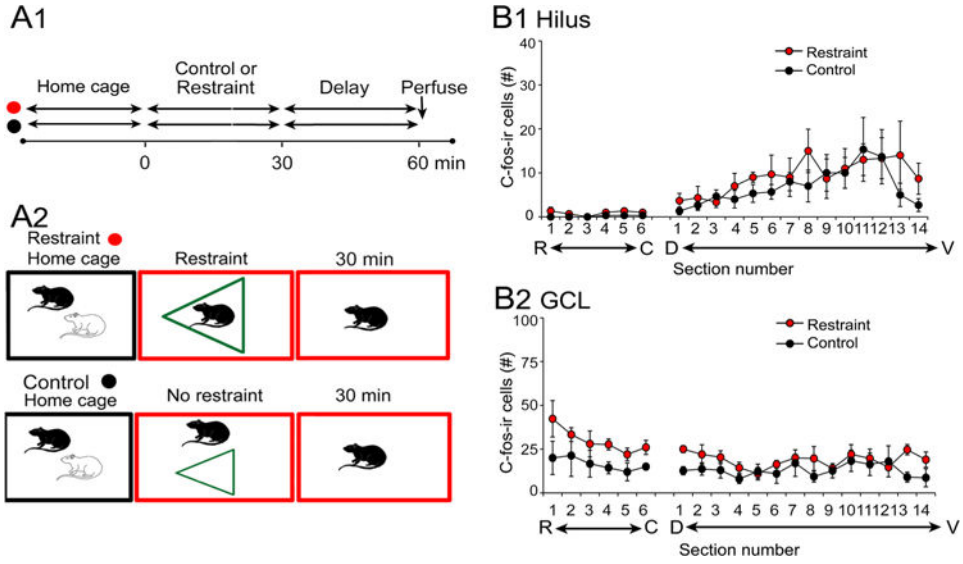

Fig. 7.

Effects of prolonged restraint on hilar and GCL c-fos-ir. **a** Schematic illustrates the two experimental groups. One group was restrained for 30 min and perfused after an additional 30 min (*red*). Another group was placed in a new cage and then perfused 60 min later. **b** There were no significant differences in hilar c-fos-ir (**1**) or GCL c-fos-ir (**2**)

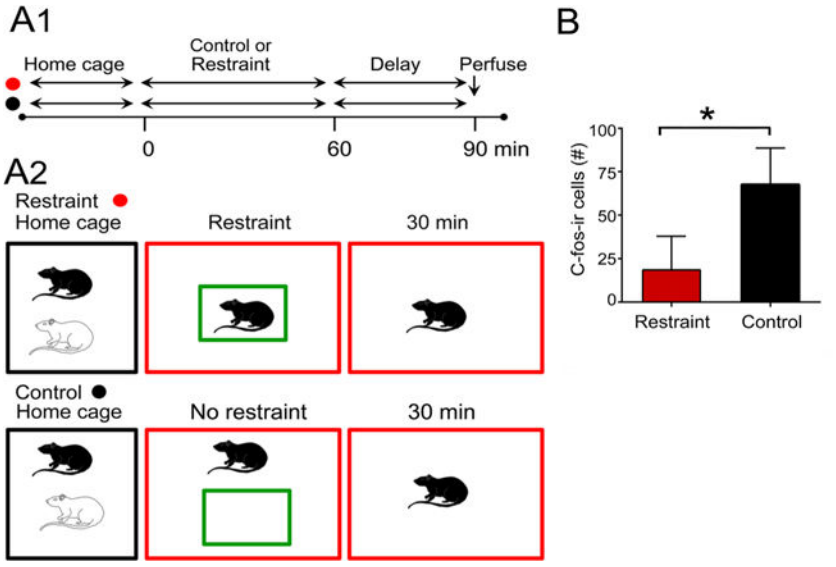

Fig. 8.

Effects of restraint in a transparent box. **a** Schematic illustrates the experimental groups. Animals either were placed in a transparent box for 30 min and then perfused after an additional 30 min (*red*) or placed in a new cage and perfused 60 min later. **b** There were significant differences in the two groups, with restrained rats showing less hilar c-fos ir

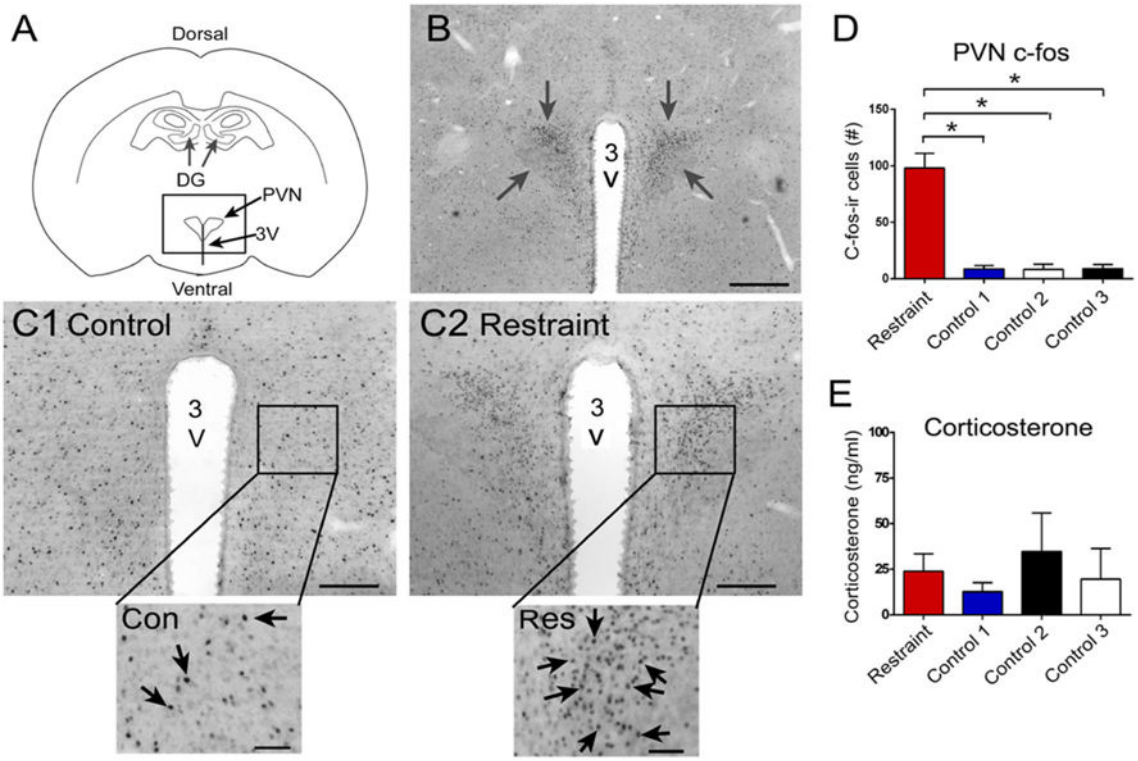

Fig. 9.

Effects of restraint on c-fos-ir of the PVN. **a** Diagram illustrates the location of the PVN. *3V* third ventricle. **b** C-fos-ir in the PVN (*arrows*) in a rat that was restrained for 10 min and perfused 30 min later. Calibration, 500 μm. **c** Comparison of PVN c-fos-ir in a rat that was a control (**1**) or restrained animal (**2**). The *boxed area* is expanded at the *bottom. Arrows* point to c-fos-ir nuclei. The control rat was from group 3 of Fig. 4a. The restrained rat was from the restrained group in Fig. 4a. Calibrations in **c1** and **c2** are the same as **b**. Calibrations in *insets*, 50 μm. **d** Comparison of c-fos-ir in the PVN showed significant differences between groups by one-way ANOVA and post hoc tests showed that the restraint group had more c-fos-ir than any of the other groups. The groups were the same as those in Fig. 4a. $*p < 0.05$. **e** Mean corticosterone levels in the four groups. Different rats from **d**. Measurements were made from serum collected after 10 min restraint or control conditions and used ELISA. There were no significant differences

Table 1

Antibody use and specificity

Primary antibody	Generation and characterization	Blocking solution	Secondary antibody
GluR2/3 Rabbit polyclonal (#AB1506, Millipore) Brightfield: 1:100 Confocal: 1:100	Raised against a synthetic peptide corresponding to the C-terminus (amino acids 864–883) of rat GluR2; this antibody recognized a 110 kDa protein on Western blot corresponding to the molecular weight of GluR2/3 (information from the manufacturer's data sheet and (Tse et al. 2008)	Brightfield: 10% normal goat serum (Vector) in 0.1 M Tris blocking solution[a] Confocal: 10% donkey serum (Sigma) in 0.1 M PB blocking solution[b]	Brightfield: goat anti-rabbit (1:400, Vector) Confocal: donkey anti-rabbit, Alexa fluor 546 (1:500, Invitrogen)
C-fos Goat polyclonal (Santa Cruz) Brightfield: 1:10,000 Confocal: 1:1000	Raised against the N-terminus peptide of human c-fos (amino acids 3–16). Western blot was used to show that the antibody recognized a 62 kDa protein corresponding to the molecular weight of c-fos (information from the manufacturer's data sheet) specificity has also been confirmed by immunoblot using a Syrian hamster embryonic cell line (Preston et al. 1996) and subsequently verified with Western blot of human T cells (Whisler et al. 1997)	Brightfield: 10% normal horse serum (Vector) in Tris blocking solution Confocal: 10% donkey serum (Sigma) in 0.1 M PB blocking solution	Brightfield: Horse anti-goat (1:400, Vector) Confocal: donkey anti-goat, Alexa fluor 488 (1:500; Invitrogen)
GAD67 Mouse monoclonal (#MAB5406, Millipore) Confocal: 1:1000	Clone 1G10.2. Raised against recombinant GAD67. "Reacts with the 67 kDa isoform of GAD67 of rat, mouse and human origins, other species not yet tested. No detectable cross reactivity with GAD65 by western blot on rat brain lysate when compared to blot probed with AB1511 that reacts with both GAD65 and GAD67" (quoted from the manufacturer's website)	Confocal: 10% donkey serum (Sigma) in 0.1 M PB blocking solution	Confocal: donkey anti-rabbit, Alexa fluor 546 (1:500, Invitrogen)
PV Mouse monoclonal (#MAB1572, Millipore) Confocal: 1:100	Raised against frog muscle PV. Western blot was used to show that the antibody recognizes a single band of 12 kDa corresponding to NPY (Information from the manufacturer's data sheet). We observed a similar pattern of labeling as described in previous reports where the antibody was characterized (Celio 1990)	Confocal: 10% donkey serum (Sigma) in 0.1 M PB blocking solution	Confocal: donkey anti-mouse, Alexa fluor 488 (1:500; Invitrogen)
NPY Rabbit polyclonal (Immunostar) Confocal: 1:100	Raised against a synthetic porcine NPY. Preabsorption of the diluted antiserum with excess NPY blocked all staining, whereas related peptides (e.g., peptide YY and avian pancreatic peptide) and somatostatin, which is colocalized in some interneurons with NPY, had no effect (information from the manufacturer's data sheet)	Confocal: 10% donkey serum (Sigma) in 0.1 M PB blocking solution	Confocal: donkey anti-rabbit, Alexa fluor 546 (1:500, Invitrogen)
Calretinin Rabbit polyclonal (#AB5054, Millipore) Confocal: 1:500	Raised against recombinant rat calretinin. Recognizes calretinin bound or unbound to calcium by western blot according to the manufacturer's website	Confocal: 10% donkey serum (Sigma) in 0.1 M PB blocking solution	Confocal: donkey anti-rabbit, Alexa fluor 546 (1:500, Invitrogen)
nNOS Rabbit polyclonal (#60870, Cayman Chemical) Confocal: 1:1000	Raised against a peptide corresponding to amino acids 1422–1433 of human nNOS	Confocal 5% donkey serum (Sigma) in 0.1 M PB blocking solution	Confocal Donkey anti-rabbit, Alexa fluor 546 (1:500, Invitrogen)

[a] 0.25% Triton X-100 and 0.005% bovine serum albumin in Tris

[b] 0.25% Triton X-100 and 0.005% bovine serum albumin in 0.1 M PB